ALKALI-SILICA REACTION OF VOLCANIC ROCKS

Zuzana Seidlová[1,2*], Richard Přikryl[1], Zdeněk Pertold[1], Šárka Šachlová[1,2]

[1]Charles University in Prague, Faculty of Science, Institute of Geochemistry, Mineralogy and Mineral Resources, Czech Republic

[2]Academy of Sciences of the Czech Republic, v.v.i., Institute of Rock Structure and Mechanics, Czech Republic

Abstract

Alkali-silica reactivity (ASR) of volcanic rocks is highly variable according to their microstructure, mineral composition, and presence of SiO_2 rich glass. The current study focused on the laboratory investigation of ASR of various types of volcanic rocks employing accelerated mortar-bar test and gel-pat test, combined with microscopic methods. Observation of ASR associated with volcanic rocks was completed by the investigation of 15 years old concrete pavements containing selected rocks.

From the wide range of studied volcanic rocks (basalts, phonolites, melaphyres, diabases) only minority showed increased ASR. In the case of felsic volcanic rocks, high ASR is connected to the presence of SiO_2 rich glass. Surprisingly, ASR was also observed in connection with one spilite. The reason for such a behavior is related to the geological origin of spilite (basalt under marine conditions), which involves extensive changes of chemical and mineral composition (e.g. albitization, chloritization) associated by migration of SiO_2.

Keywords: Alkali-silica reaction, volcanic rocks, polarising microscopy, SEM/EDS.

1 INTRODUCTION

Over the past two decades, three major projects have been implemented to determine the alkali-silica reactivity (ASR) potential of aggregates used in concrete in the Czech Republic [1,2,3]. Additionally, new standard methods are being tested, and their possible application to Czech aggregates was verified [4].

Alkaline conditions increase solubility of various types of silica present in aggregates. SiO_2 reacts with hydroxyl ions forming silanol and siloxane groups. Increasing pH increases extent of the reaction. Polymerization of silanol and siloxane groups leads to the formation of alkali-silica gel (ASG). ASG can absorb water molecules and swells [e.g. 5,6]. The progressive formation of ASG causes cracking inside the aggregates and cement paste. There are often obvious cracks on the surface of aggregates. Monitoring the expansion rate of construction is essential for structural integrity assessment. For this purpose, there were developed many techniques, such as long-term measurement of length changes between deliberate reference points on the concrete surface. This measurement should represent the entire structural element [e.g. 7]. Spalling and ASG on the concrete surface may also be a symptom of the ASR, but it does not demonstrate excessive expansion of concrete [5]. The presence of ASG on the concrete surface indicates the existence of the ASR. ASR can be associated by colour changes visible along the ASR cracks in concrete [8]. The degree of ASR is slow and external signs such as ASG, spalling, cracking and net volume changes may not be evident for many years. In some rare cases, ASG formation occurred, but did not indicate the failure. However, in many cases, ASG formation is accompanied by a failure of the structures due to generated expansive forces [5,7,9].

Many methods have been proposed in the last few years to assess whether the components of aggregates and concrete mixtures are prone to the formation of ASR. The reactivity of aggregates is provided by microscopic methods (polarising microscopy, scanning electron microscopy combined with energy dispersive spectrometer – SEM/EDS method), chemical tests and expansion (mortar-bar and concrete prism) tests [5,10].

---

* Correspondence to: themen@centrum.cz

The most reliable way of determining the susceptibility of aggregates to ASR is to verify the reactivity of aggregate in practice. This verification can be done by inspection of concrete structures existing 10 years or more [5]. Series of tests were designed to evaluate resistance of aggregate or a combination of cement and aggregates to the action of alkalis. Typically, these tests are intended to evaluate new aggregate sites [11]. Acid volcanic rocks, containing higher content of SiO_2 (amorphous or cryptocrystalline SiO_2, very fine-grained quartz) are prone to ASR. The basic and mafic volcanic rocks are generally safe in this respect. However, the situation could be different with spilites. Spilites (resp. basalts) are originally composed of basic plagioclase and pyroxene. Their secondary interaction with seawater changes their character into acid [12].

Spilitization of basalts is a complex reaction that involves mineralogical, chemical and sometimes also structural changes. The feldspar (plagioclase) is subjected to the albitization. Mafic minerals (pyroxene, amphibole) are chloritized producing newly formed chlorite, calcite, epidote, chalcedony, prehnite, or other low-temperature hydrous crystallization products [e.g. 13].

Chemically, the main changes are intake of Na^+ and H_2O, and release of Ca^{2+} and SiO_2. Chloritization of mafic minerals (pyroxenes and amphiboles) is accompanied by the release of SiO_2 and intake of Al_2O_3. Spilitization could proceed from incipient to complete stages. Fragmented rock types, like agglomerates, tuffs, amygdaloidal rocks etc. react more readily. The great amount of SiO_2 generated during spilitization escapes from the rocks to form bodies of siliceous cherts in open geological systems, or remain in spilitic rocks as quartz, micro- to crypto-crystalline quartz, and chalcedony grains, replacements, impregnation etc [e.g. 14]. Especially these forms of SiO_2 are usually alkali silica reactive. Because of very different mineralogical composition of spilites, they deserve detailed study in relation to ASR.

Volcanic rocks are widely used in the Czech Republic as crushed aggregate (34 % of total crushed stone production). Various volcanic rocks (13 basalts, 5 spilites, 4 melaphyres, 2 phonolites, 1 rhyolite, and 1 diabase) were investigated with the aim to quantify their ASR potential experimentally and to compare it with ASR originating in real concrete samples. Experimental methods consisted of standard laboratory tests (accelerated mortar bar test and gel pat test) improved by microscopic techniques (polarising microscopy, SEM/EDS, image analysis). Concrete samples were subjected to microscopic investigation. Alkali-silica reactive aggregates were distinguished on the base of their spatial relationship with ASG. Possible effect of spilitisation on ASR was documented based on variable alkali-silica reactivity of spilite-like samples.

2 EXPERIMENTAL METHODS

2.1 Samples

Samples were selected based on the following criteria: (1) the rocks are of volcanic origin located in the Bohemian Massif (Czech Republic, Tab. 1); and (2) rocks are quarried and used in construction industry. Selected samples were petrographically classified as: basalt, spilite, diabase, melaphyre, porphyry, phonolite, and rhyolite.

2.2 Concrete samples

Four different sets of samples were selected: samples from Highway No.D1 (37 - 45 km from Prague); samples from Highway No.D5 (128 km from Prague); samples from the Highway No.D11 (16 - 18 km from Prague); as well as samples from the Vrbová Lhota rest area (D11-VL, situated 36 km from Prague). Concrete samples (drill cores with diameters of 80 and/or 150 mm) were taken, representing portions of those concrete pavements indicating both the most extensive, as well as the least extensive deterioration [15].

2.3 Accelerated mortar bar test

Accelerated mortar bar test (following the standard ASTM C1260, [16]) was used with the aim to quantify the potential ASR of aggregates. The samples were crushed and sieved into the fraction 0/4 mm. Three different mortar bar specimens were prepared from each sample using the fraction 0/4, mm and tested in 1M NaOH solution at 80°C. Expansion of mortar bar specimens was measured for fourteen days testing period. The test was performed in cooperation with ZKK, Ltd.

2.4 BS 7943

The gel pat test [17] was originally designed to identify amorphous silica-rich aggregates, exhibiting rapid ASR in concrete and mortar. It enables detection of the ASR aggregates reactive in a special type of cement. The gel pat test method was performed in the Geochemical Laboratory (Charles University in

Prague, Faculty of Science). It consisted of: (1) sample preparation (separation of the fraction 2/4 mm); (2) cement paste preparation (using distilled water and Portland cement CEM I 42.5 equaling to the ratio 0.4); (3) gel pat specimen preparation (filling of the steel mould by aggregates and cement paste); (4) gel pat specimen hardening for 24 hours; (5) gel pat specimen testing in plastic containers in 2M (NaOH + KOH) solution at room temperature for 14 – 20 days; and (6) macroscopic examination (Figure 1).

2.5 Polarising microscopy

The petrographic study of rocks and rock-like materials by microscopic technique constitutes an important part of aggregate ASR testing [18], as well as the investigation of concrete deterioration [2,5,19,20]. Polarising microscopy was performed in the Laboratory of microscopic techniques (Charles University in Prague, Faculty of Science) using thin sections prepared from mortar bar specimens (2 sections for each specimen), from gel pat test specimens (2 sections per each specimen), and from concrete samples (4-8 thin sections from each drill core) with the aim of identifying: I) the identification of the aggregate type, II) the relationship between aggregate and cement paste, and III) the type and location of voids and features related to the presence of ASR.

2.6 SEM/EDS method

The SEM/EDS analysis enabled determination of the chemical composition of phases, e.g. identification of very-fine grained and accessory minerals in aggregates, and identification of ASG. The uncovered polished thin sections were coated in a Carbon atmosphere. A Cambridge Cam Scan S4 electron microscope with Oxford Instruments LINK ISIS 300 energy dispersive analytical system was used (Laboratory of Electron Microscopy and Microanalysis, Charles University in Prague). The measurement was carried-out under the following conditions: beam current 3 nA, accelerating voltage 20 KV, with a 100 nm resolution. A SPI Supplies 53 Minerals Standard set 02753-AB was used for routine quantitative calibration. The detection limit is 0.5 wt.%.

2.7 Image analysis

The system of petrographic image analysis employed in this study consisted of manual image pre-processing, computer image analysis, and data evaluation (Figure 2). Image pre-processing involves: capturing of the image by means of conventional or digital photography in an optical microscope, identification of the measured objects (i.e. petrographic type of the fragments), and image modification using graphic software with a final image resolution of 300 dpi (Corel Draw v. 12.0). The image modification is a crucial point in the image pre-processing, because the software used (SIGMASCAN Pro by Jandel Scientific) requires a binary image in which the object is differentiated from the background based on the intensity along a grey scale. This means that the object must either be "lighter" or "darker" than the background. In the preparatory stage, it is also important to add an identifier to each object, indicating its petrographic nature. This identification is necessary for multiphase materials, such as the concrete samples studied. The analysis of multiphase materials requires measurement of an appropriate number of objects, which ranges from 200 to 300 per sample. Using SIGMASCAN Pro software, the image measurement is performed by a feature-specific approach (i.e. fill measurement). In practice, the objects are measured separately. After the measurement, each object is filled with a contrasting colour, in order to avoid multiple analyses of an already-measured grain. Finally, the data obtained are analysed using any kind of statistical software. The measurement included volume of ASG (in all types of samples) and volume of aggregates, cement paste and pore voids (in concrete samples). More details concerning image preparation and analysis can be found elsewhere [2,21].

3 RESULTS

3.1 Characterisation of the volcanic rock types

Basalt - a dark-coloured, very fine-grained to fine-grained (10 – 50 μm), volcanic rock composed mainly of Na-rich plagioclase (containing minor content of potassium) and pyroxene minerals (augite). Oxides rich of Mg^{2+}, Fe^{2+}, Fe^{3+}, and Ti^{4+} and apatite were identified in accessory amount (see Figure 3a).

Phonolite - a very fine-grained to fine-grained (50 – 250 μm) volcanic rock, mainly composed of abundant feldspathoids (nepheline, analcime) and K-feldspar and rare albite. Pyroxene (augite, aegirine-augite) represents the most common mafic mineral. Titanite, magnetite, ilmenite and Fe-hydroxides were identified in accessory amount (see Figure 3b).

Melaphyre - a medium-to-dark-coloured, very fine-grained to medium-grained (10 – 500 μm) volcanic rock mainly composed of plagioclase, alkali-feldspars and pyroxene (augite). Fine-grained SiO_2 fills small voids. Magnetite and ilmenite form small inclusions.

Spilite - a very fine-grained to fine-grained (5 – 200 μm) volcanic rock, resulting particularly from alteration of oceanic basalt, composed of plagioclase (from albite to andesine), chlorite, epidote, and amphibole (actinolite). Spilite sample No. 25 was found enriched of very fine-grained SiO_2 included in the matrix. Quartz and carbonates were analysed filling veins 0.1 – 0.5 mm wide (see Figure 3c).

Rhyolite - a very fine-grained to fine-grained (10 – 100 μm) volcanic rock, of felsic composition, having a texture from glassy to aphanitic and porphyric. Quartz, alkali feldspar and plagioclase are the main minerals. Quartz also forms porphyric clasts 100 - 200 μm large. Biotite, sericite, apatite, zircon and xenotime are common accessory minerals (see Figure 3d).

Diabase - a fine-to-medium-grained (100 – 500 μm) volcanic rock, composed of plagioclase crystals set in a finer matrix of pyroxene (augite). Magnetite and ilmenite were analysed in accessory amount.

3.2 ASR according to the accelerated mortar bar test and gel pat test

Accelerated mortar bar test revealed expansion values varying between 0 - 0.282 % (Table 2). The lowest expansion values were indicated by basalt, phonolite and diabase samples. The highest (and anomalous) expansion value was found in connection with spilite sample No.25.

Microscopic investigation enabled us to quantify the volume of ASG in mortar-bars and gel-pats (Table 2). The total volume of ASG does not exceed 0.64 vol.% in mortar-bars and 0.103 vol.% in gel-pats. The highest volume of ASG was indicated by sample No.21 in mortar-bars and No.25 in gel-pats.

3.3 ASR of volcanic rock types observed in concrete samples

Coarse aggregates (particles with a diameter > 4 mm) and fine aggregates (with a diameter < 4 mm) represent the main component of concrete (forming 61.0 – 66.4 vol.% of sum total of the drill cores). The volume of cement paste did not exceed 35.1 vol.%. The total volume of pore voids varied between 4.5 - 5.0 vol.%. The volume of ASG (resp. to the microcracks) varied from between 0.1 and 1.7 vol.% (resp. 0.0 and 1.9 vol.%, see Table 3).

Coarse aggregates (forming about 40 vol.%) are composed of four dominant rock types: (a) biotite amphibole granodiorite; (b) basic volcanic rock types (e.g. basalt, spilite, and basic volcanic tuff); (c) "acid" volcanic rock types (e.g. quartz and feldspar rich tuff, tuffite, tuffitic greywacke, dacite, rhyolite); and (d) quartz aggregates (quartz particles containing more than 95% of quartz, see Tab.4). Both metamorphic rock types (e.g. amphibolite) and sedimentary rock types (e.g. limestone) are only minor constituents. The observed rock types in the investigated samples were classified according to Gillespie and Styles [22], Hallsworth et al. [23], and Robertson [24]. Fine aggregates (forming about 20 vol. %) are mainly composed of quartz, feldspar, quartz-feldspar aggregates, and plutonic and volcano-sedimentary rock types. Plutonic and volcano-sedimentary rocks identified in the fine aggregates show petrographic characteristics similar to those from the coarse aggregates, indicating their similar origin.

Microcracks were observed mainly penetrating aggregates, cement paste, and the aggregate/cement paste boundaries. ASG fill both pores and microcracks. The volume of the microcracks (resp. ASG) was accepted as the quantitative parameter reflecting the degree of the concrete's deterioration. Special attention was paid to the ASG spatially connected to the aggregates of volcanic origin. The highest amount of ASG was found connected to the quartz-and-feldspar-rich tuff, tuffite, tuffitic greywacke, dacite, rhyolite, which can be easily explained by acid character of aggregates. In contrast, basic volcanic rock types (e.g. spilite and basic volcanic tuff, investigated in the concrete from the highway No.D5) showed no signs of ASR (Figure 4a, 4b).

4 DISCUSSION

4.1 ASR under laboratory conditions compared with concrete samples

Laboratory and concrete samples were compared in our study. Two spilite samples (sample No. 20 and 25) were found in concrete samples. The spilite sample No.20 ("non reactive" spilite) forms more than

30 vol. % of concrete from the highway No D5. The spilite sample No.25 ("reactive" spilite) forms 18.5 – 37.9 vol. % of concrete from the highways Nos.D1, D11 and D11-VL. Spilite sample No.20 showed no influence on ASR in both concrete and mortar samples. In contrast, spilite sample No.25 showed positive correlation to the presence of ASG and microcracks (see Table 3 and 4) in concrete samples as well as high ASR potential measured according to the expansion of mortar bars (Table 5).

4.2 Effect of the spilitization on ASR of volcanic rocks

"Non reactive" spilite No.20 is mainly composed of plagioclase (andesine to labradorite), pyroxene and amphibole indicating no minerals or phases deleterious to ASR. No signs of spilitization were found in this sample.

"Reactive" spilite was probably subjected to spilitisation connected to the albitization, and to the formation of chlorite, SiO_2-rich accumulations as well as quartz-rich veins (Figure 5). The formation of SiO_2-rich accumulations can explain anomalous ASR of this sample. SiO_2-rich accumulations can exist within the spilite quarry. Both spilite and SiO_2-rich parts of the quarry are mixed within the bulk system of quarrying. Spilite-like aggregate contaminated of SiO_2 represents aggregate responsible to the ASR.

5 CONCLUSIONS

Volcanic rocks (basalt, diabase, phonolite) show low degree of ASR under laboratory conditions as well as in real concrete samples. Medium degree of ASR was found in connection to the "acid" volcanic rocks such as rhyolite and melaphyre. Spilite samples indicated low degree of ASR in four from five samples. Only one spilite sample indicated anomalous ASR (seven times higher compared to other spilites). There is expected effect of spilitization in the case of this sample. This can be due to the formation of SiO_2-rich accumulations, veins and dykes which can be deleterious due to ASR.

Application of microscopic methods on mortar specimens and real concrete samples enabled to identify deleterious components in the samples generally regarded to be safe due to ASR (SiO_2-rich parts in spilite). This can be important especially in the case of new projects planning to use crushed volcanic rocks in outdoor concrete constructions.

Acknowledgements

This study was financially supported from the research project "Creating a database for measuring properties of rocks used for the production of crushed stone" provided by the Ministry of Environment of the Czech Republic. Financing from the Projects Nos. MSM0021620855, SVV 263203, P104/12/0915 and 103/09/P139 is also acknowledged.

6 REFERENCES

[1] Modrý, S, Dohnalem, J, Fenrich, J, Hrbe, M, Táborský, T, and Dobiáš, D (2003): Elimination of alkali reactivity of aggregates in concrete in highway constructions. Unpublished technical report. Czech Technical University in Prague (In Czech).

[2] Lukschová, Š, Přikryl, R, and Perold, Z (2009): Evaluation of the alkali-silica reactivity potential of sands. Magazine of Concrete Research (61): 645-654.

[3] Pertold, Z, Lukschová, Š, Přikryl, R, Burdová, A, Seidlová, Z, and Šťastná, A (2010): Causes and extent of failures cement-concrete pavement caused by the housing AAR. (In Czech).

[4] Šachlová, Š (2011): Aggregates affected by ASR in mortar bar and gel pat specimens. Proceedings of the 33rd International Conference on Cement Microscopy. 17.-21.4.2011, USA, San Francisco.

[5] St John, DA, Poole, AB, and Sims, I (1998): Concrete petrography. A handbook of investigative techniques. Arnold Publishers. London. 474.

[6] Bulteel, D, Rafai, N, Degrugilliers, P, and Garcia-Diaz, E (2004): Petrography study on altered flint aggregate by alkali-silica reaction. Materials Characterization: (53): 141-154.

[7] Bennet, DL (2004): Handbook for Identification of Alkali-Silica Reactivity in Airfield Pavements. U.S. Department of Transportation, Federal Aviation Administration.

[8] Fernandes, I, Noronha, F, and Teles M (2007): Examination of the concrete from an old Portuguese dam: Texture and composition of alkali-silica gel. Materials Characterization (58): 1160-1170.

[9] Wang, H, and Gillott, JE (1991): Mechanism of alkali-silica reaction and the significance of calcium hydroxide. Cement and Concrete Research (21): 647-654.

[10] Korkanc, M, and Turgul A (2005): Evaluation of selected basalts from the point of alkali-silica reactivity. Cement and Concrete Research (35): 505-512.

[11] Stark, DC (1994): Alkali-Silica Reaction in Concrete In Significance of Tests and Properties of Concrete and Concrete-Making Materials. ASTM STP 169 C, P. Klieger and J. Lamind, eds., 365-371.

[12] Arghe, F, Skelton, A, and Pitcairn I (2011): Spatial coupling between spilitization and carbonation of basaltic sills in SW Scottish Highlands: evidence of a mineralogical control of metamorphic fluid flow. Geoflids (11): 245–259.

[13] Graser G, Markl G (2008): Ca-rich ilvaite-epidote-hydrogarnet endoskarns: a record of late-magmatic fluid influx into the persodic Ilmaussaq complex, South Greenland. Journal of Petrology 49(2): 239-265

[14] Paradis, S, Taylor, B Watkinson, DH, Jonasson, IR (1993): Oxygen-isotope zonation and alteration in the Northern Noranda district, Quebec – evidence for hydrothermal fluid-flow. Economic Geology and the Bulletin of the Society of Economic Geologist (88): 1512-1525.

[15] Šachlová Š., Burdová A., Pertold Z., Přikryl R. (2011). Macro- and micro-indicators of ASR in concrete pavement. Magazine of Concrete Research (63): 553-571.

[16] ASTM C1260-07 (2011): Test Method for Potential Alkali Reactivity of Aggregates (Mortar-Bar Method). American Society for Testing and Materials, West Conshohocken, Volume 04.02.

[17] BS 7943 (1999): Interpretation of petrographic analysis of aggregates in ASR. British Standards Institution, London, UK.

[18] RILEM (2003): AAR-1 - Detection of potential alkali-reactivity of aggregates – petrographic method. Materials & Structures (36): 480-496.

[19] Clark, BA, Swoeble, AJ, Lee, RJ, and Skalny, J (1992): Detection of ASR in opened fractures of damaged concrete. Cement and Concrete Research (22): 1170-1178.

[20] Koskiahde, A (2004): An experimental petrographic classification scheme for the condition assessment of concrete in façade panels and balconies. Materials Characterization (53): 327- 334.

[21] Přikryl, R (2001): Some microstructural aspects of strength variation in rocks. International Journal of Rock Mechanics and Mining Sciences (38): 671 – 682.

[22] Gillespie, MR, and Styles, MT (1999): BGS Rock Classification Scheme. Classification of igneous rocks. British Geological Survey Report (1): 54.

[23] Hallsworth C.R., Knox R.W.O.B. (1999): BGS Rock Classification Scheme. Classification of sediments and sedimentary rocks. British Geological Survey (3): 46.

[24] Robertson S (1999): BGS Rock Classification Scheme. Classification of metamorphic rocks. British Geological Survey (2): 26.

TABLE 1. The list of investigated samples.

Rock type	S. No.	Quarry	Rock type	S. No.	Quarry
Basalt	CZ 13	Krásný Les	Spilite	CZ 20	Trnčí
Basalt	CZ 14	Císařský	Spilite	CZ 22	Čenkov
Basalt	CZ 16	Těchlovice	Spilite	CZ 25	Zbraslav
Basalt	CZ 27	Dolánky	Spilite	CZ 26	Sýkořice
Basalt	CZ 28	Dobkovičky	Spilite	CZ 44	Zahrádka
Basalt	CZ 31	Všechlapy	Melaphyre	CZ 17	Libeč - Babí
Basalt	CZ 32	Měrunice	Melaphyre	CZ 18	Doubravice
Basalt	CZ 33	Chaberce	Melaphyre	CZ 24	Rožmitál
Basalt	CZ 34	Smrčí	Melaphyre	CZ 35	Bezděčín
Basalt	CZ 36	Mokrá	Phonolite	CZ 15	Mariánská skála
Basalt	CZ 37	Číhaná	Phonolite	CZ 38	Chlum
Basalt	CZ 41	Děpoltovice	Rhyolite	CZ 21	Těškov
Basalt	CZ 42	Úhošťany	Diabase	CZ 23	Chrtníky

TABLE 2. Comparing of the Expansion, presence of ASG in mortar-bars (MBS) and in gel-pats (GP) in different Rock types.

Rock type	Expansion 14-days (%)	ASG (MBS, vol. %)	ASG (GP, vol. %)
basalt	0.000 - 0.024	0.00 - 0.3	0.00 - 0.24
spilite	0.001 - 0.035 0.282*	0.00 – 0.59	0.00 - 0.103
melaphyre	0.069 - 0.127	0.00 – 0.64	0.00 - 0.033
phonolite	0.002 - 0.011	0.00	0.00
rhyolite	0.15	0.45 – 0.61	0.00 - 0.17
diabase	0.04	0.00	0.03 - 0.17

* Sample No. CZ 25 indicating anomalous expansion compared to other spilite samples.

TABLE 3. Composition of concrete (vol. %, calculated as an average value of 4 – 6 drill cores). CP – cement paste, agg – aggregates.

Drill core no.	CP	Pores	ASG	Micro-cracks	Coarse agg.	Fine agg.	Total
D11	27.2	4.8	0.5	1.0	45.3	21.1	100.0
D11-VL	30.4	5.0	1.7	1.9	40.5	20.5	100.0
D1	29.3	4.6	0.4	0.8	42.5	22.3	100.0
D5	35.1	4.5	0.1	0.0	41.4	18.9	100.0

TABLE 4. Composition of aggregates in concrete. (vol. %). V.r. – volcanic rock; q-f. – quartz-and-feldspar-rich; bt.a. - biotite-amphibole-rich; grd. – granodiorite; bt. – biotite-rich; Q – monomineral quartz; f – monomineral feldspar; n.a. – not analyzed.

Drill core no.	Basic v.r.	Acid v.r.	Granite	Bt.a. grd.	Bt. grd.	Amphi-bolite	Lime-stone	Q-f. agg.	Q	F
D11	0.0	37.9	0.6	0.0	0.0	5.1	0.0	12.0	10.5	0.4
D11-VL	0.0	31.2	9.2	0.0	0.0	0.0	0.0	7.6	13.2	0.0
D1	0.0	18.5	0.0	25.1	0.0	0.0	0.0	9.5	11.1	0.7
D5	33.4	0.0	0.0	0.0	0.0	0.0	2.0	3.2	21.1	0.6

TABLE 5. Comparison between of the samples in experimental conditions and in Highway concrete samples.

Rock type	ASR in experimental conditions	ASR in concrete	Alkali-silica reactive components
basalt	low	not documented	-
"non reactive" spilite *"reactive" spilite	low *very high	low *very high	no q-f-rich fine-grained matrix
melaphyre	medium	not documented	
phonolite	low	not documented	-
rhyolite	medium	not documented	
diabase	low to medium	not documented	

* Sample No. CZ 25 indicating anomalous results compared to other spilite samples.

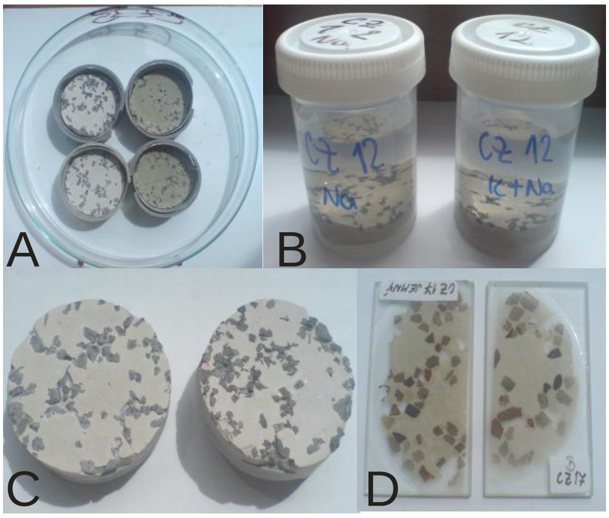

FIGURE 1. Schematic illustration of gel pat test. A – gel pat specimen preparation; B – gel pat specimen testing in alkaline solution; C – gel pat specimens after the testing perion; D – thin sections prepared from gel pat specimens.

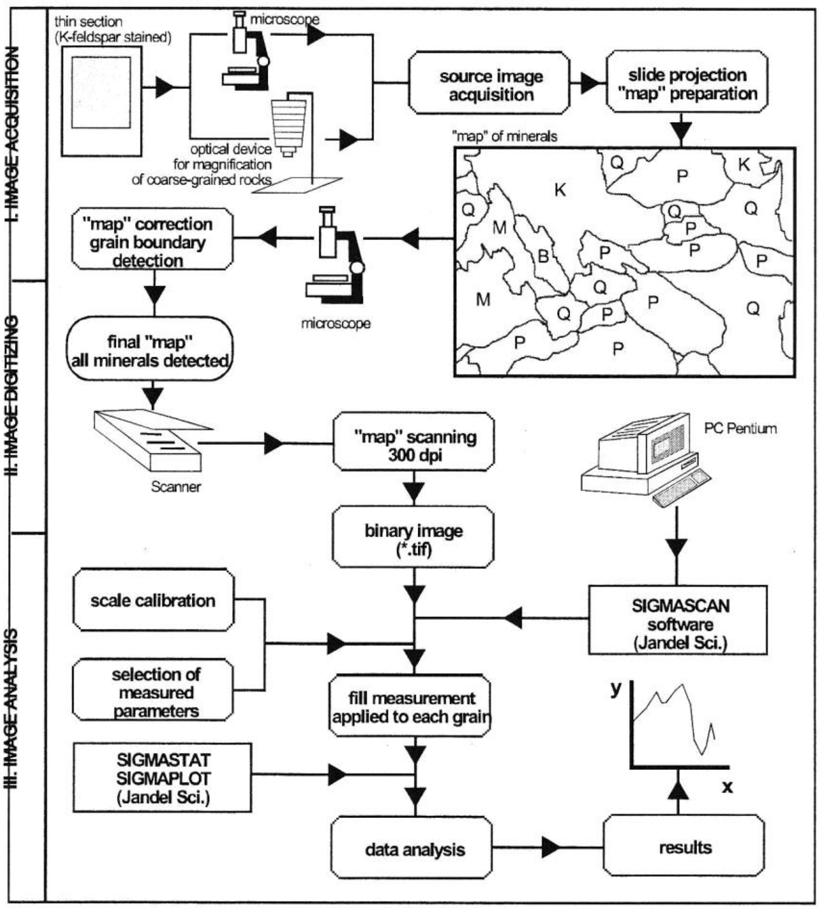

FIGURE 2. Schematic diagram of Image analysis [21].

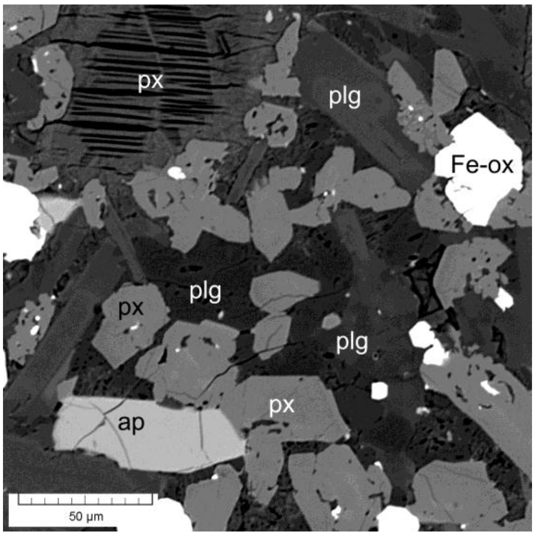

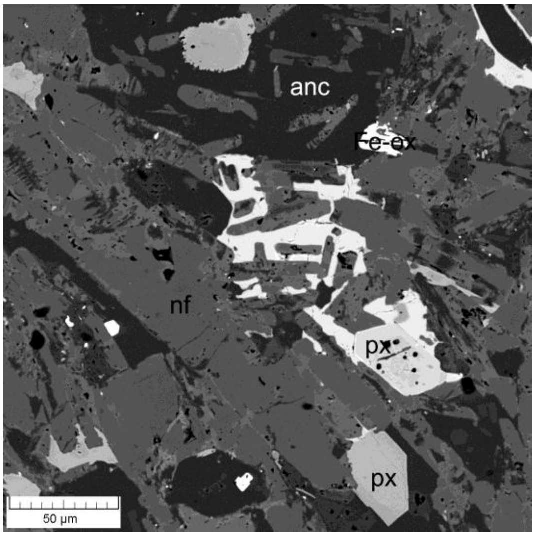

FIGURE 3a. (on the left) Basalt sample No. 34 composed of plagioclase (plg), pyroxene (px), apatite (ap) and Fe-oxide (Fe-ox). SEM/EDS method, BSE image.

FIGURE 3b. (on the right) Phonolite sample No. 38 composed of feldspathoids (analcime – anc, nepheline - nf) and pyroxene (px). SEM/EDS method, BSE image.

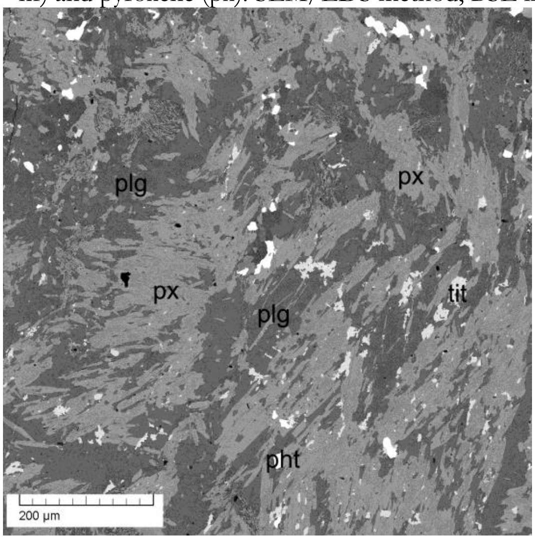

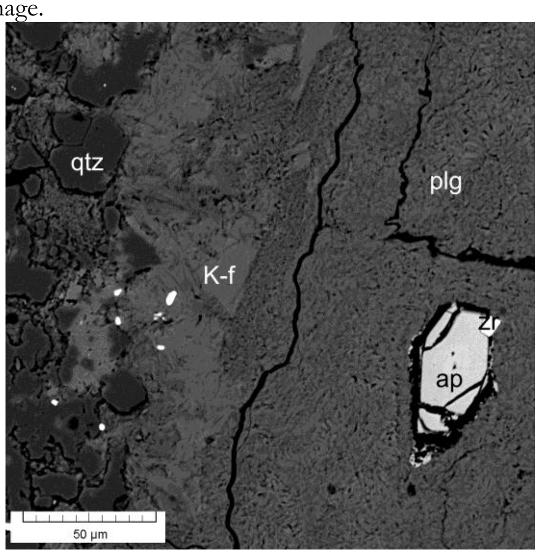

FIGURE 3c. (on the left) Spilite sample No.20 composed of plagioclase (plg) and pyroxene (px). Pyrhotite (pht) was identified in accessory amount. SEM/EDS method, BSE image.

FIGURE 3d. (on the right) Rhyolite sample No.21 composed of plagioclase (plg), quartz (qtz), and K-feldspar (K-f). Apatite (ap) and zircon (zr) form small inclusions. SEM/EDS method, BSE image.

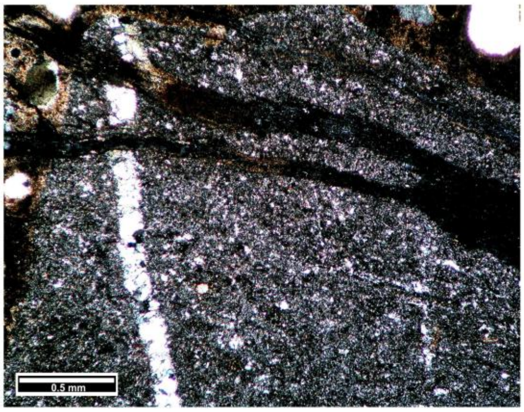

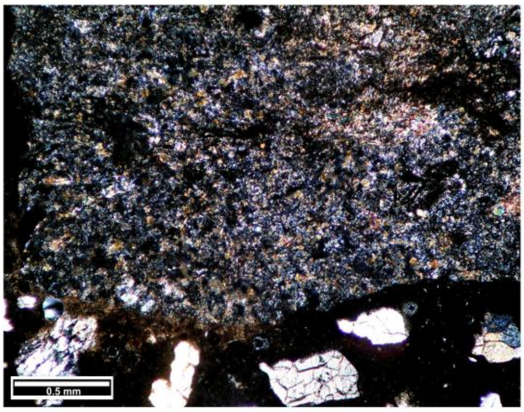

Figure 4a. (on the left) “Reactive” spilite observed in concrete samples from the highway No.D11 penetrated by ASR microcracks. Polarising microscope, crossed nicols.
Figure 4b. (on the right) “Non reactive” spilite observed in concrete samples from the highway No. D5 indicating no signs of ASR. Polarising microscope, crossed nicols.

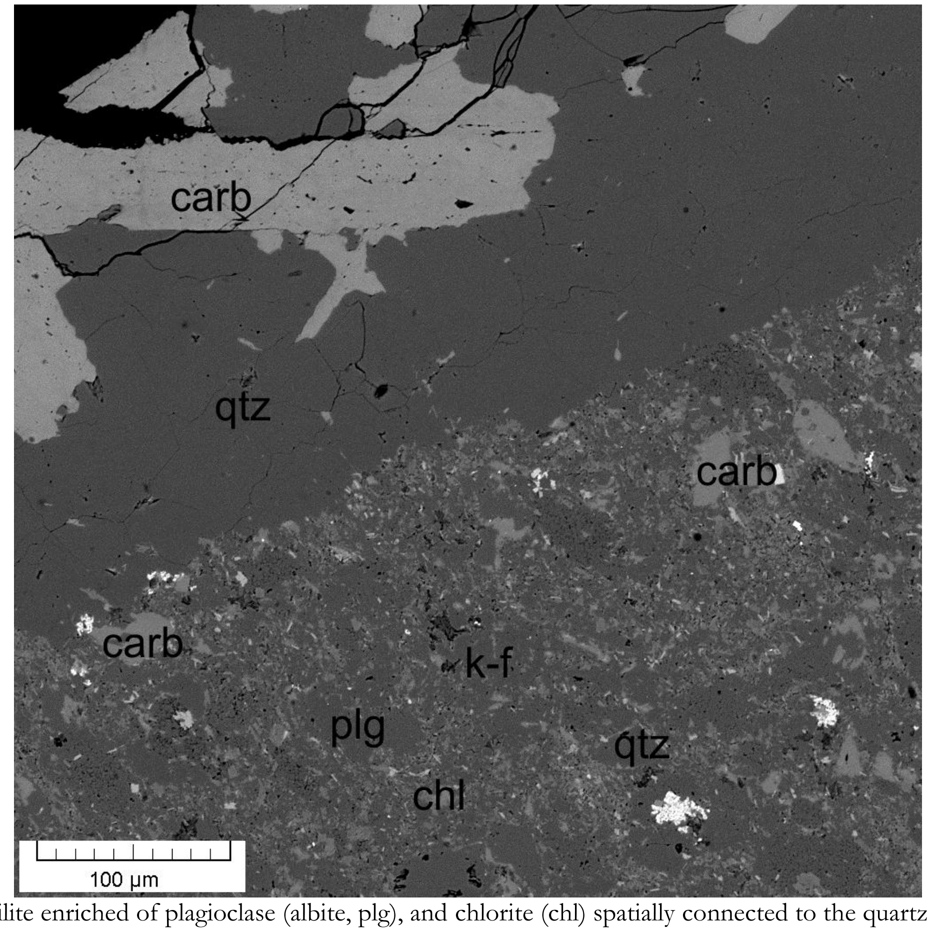

Figure 5. Spilite enriched of plagioclase (albite, plg), and chlorite (chl) spatially connected to the quartz and carbonate (carb) vein. SEM/EDS method, BSE image.